Fundamentals of Contemporary Mathematical Sciences
doi:10.54974/fcmathsci.1398394
(**2024**) **5**(2) 143 – 158
Research Article

A New Numerical Simulation for Modified Camassa-Holm and Degasperis-Procesi Equations via Trigonometric Quintic B-spline

İhsan Çelikkaya *
Batman University, Faculty of Science and Art, Department of Mathematics
Batman, Türkiye

Received: 01 December 2023 **Accepted:** 05 July 2024

Abstract: In this study, the soliton solutions of the modified Camassa-Holm (mCH) and Degasperis-Procesi (mDP) equations, known as modified b-equations with significant physical properties, have been obtained. The movement and positions of soliton waves formed by solving the mCH and mDP equations are calculated. Ordinary differential equation systems have been derived using trigonometric quintic B-spline bases for the derivatives in the position and time directions to obtain numerical solutions. An algebraic equation system is then created by applying Crank-Nicolson type approximations for time and position-dependent terms. The stability analysis of this system has been examined using the von Neumann Fourier series method. L_2, L_∞, and absolute error norms are used to measure the convergence of the numerical results to the real solution. The calculated numerical results have been compared with the exact solution and some studies in the literature.

Keywords: Modified Camassa-Holm, modified Degasperis-Procesi equation, soliton waves, trigonometric quintic B-spline bases, collocation method.

1. Introduction

Nonlinear partial differential equations have important applications in science, such as engineering and physics. Often, it is not easy to solve a nonlinear partial differential equation analytically. Therefore, mathematicians and engineers need to obtain numerical solutions to such equations. The structures of Camassa-Holm (CH) [4] and Degasperis-Procesi (DP) [5] equations, which have many physical properties, are as follows:

$$U_t - U_{xxt} + 3UU_x - 2U_xU_{xx} - UU_{xxx} = 0, \tag{1}$$

$$U_t - U_{xxt} + 4UU_x - 3U_xU_{xx} - UU_{xxx} = 0. \tag{2}$$

*Correspondence: ihsan.celikkaya@batman.edu.tr
2020 *AMS Mathematics Subject Classification*: 65L60, 65M06, 76M10, 65L80

CH (1) and DP (2) equations are not only bi-Hamiltonian but are also linked to the isospectral problem [12]. The (1) and (2) equations are formally integrable according to the scattering / inverse scattering approaches, as well as peakon solitary wave solutions. Although both equations are similar, they are quite different in terms of the isospectral problem. The CH (1) equation accepts second-order isospectral solution while the DP (2) equation accepts third-order isospectral solution [12, 25]. The CH (1) and DP (2) equations are both integrable equations that model shallow water dynamics [18]. In this study, the numerical solutions of the equation called b-equation are obtained by modifying the convection UU_x term in the equations (1) and (2) as U^2U_x. The b-equation family is given by Wazwaz [18] in the form

$$U_t - U_{xxt} + (b+1)U^2U_x - bU_xU_{xx} - UU_{xxx} = 0. \tag{3}$$

The equation (3) gives mCH for $b = 2$ and mDP for $b = 3$ respectively. Wazwaz obtained analytical solutions of the mCH and mDP equations for $b = 2, 3$ in [18, 19], respectively, using the sine-cosine and extended tanh methods as follows:

$$U_t - U_{xxt} + 3U^2U_x - 2U_xU_{xx} - UU_{xxx} = 0,$$

$$U(x,t) = -2\sec h^2(\frac{x}{2} - t)$$

and

$$U_t - U_{xxt} + 4U^2U_x - 3U_xU_{xx} - UU_{xxx} = 0,$$

$$U(x,t) = -\frac{15}{8}\sec h^2(\frac{x}{2} - \frac{5t}{4}).$$

Obtaining both analytical and numerical solutions to such nonlinear partial differential equations is a scientifically important task. Zhou [25] investigated how the solution's derivative blows up in finite time for the Degasperis-Procesi equation. Wazwaz [18] established new solitary wave solutions for mCH and mDP using the extended tanh method. Wazwaz [19] used the tanh method and the sine-cosine method to get solitary wave solutions to the mCH and mDP equations. Abbasbandy [1] applied the homotopy analysis method to obtain the soliton wave solutions for the mCH and mDP equations. Ganji et al. [6] studied Adomian's decomposition method to solve the mCH and mDP equations. Manafian et al. [11] constructed solitary wave solutions of the mCH and mDP equations via the generalized (G'/G)-expansion and generalized tanh-coth methods. Liu and Ouyang [8] found bell-shaped solitary wave and peakon coexist for the same wave speed for the mCH and mDP equations. Lundmark and Szmigielski [10] presented an inverse scattering approach for computing n-peakon solutions of the DP equation. Yousif et al. [20] obtained solitary wave solutions of the mCH and mDP equations by the variational homotopy perturbation

method. Behera and Mehra [3] applied the wavelet-optimized finite difference method to solve the mCH and mDP equations. Wang and Tang [17] obtained four new exact solutions for the mCH and mDP equations using some particular phase orbits. Wasim et al. [16] solved mCH and mDP equations numerically by the collocation finite difference scheme based on Quartic B-spline. Yusufoğlu [21] investigated the mCH and mDP equations' analytic treatment using the Exp-function method. Zada and Nawaz [22] introduced an optimal homotopy asymptotic method for finding the approximate solutions of the mCH and mDP equations. Zhang et al. [23] applied the homotopy perturbation method directly to obtain solitary wave solutions of mCH and mDP equations. Zhang et al. [24] investigated the mCH and mDP equations via the auxiliary equation method. They obtained smooth solitary wave solutions, peakons, singular solutions, periodic wave solutions, and Jacobi elliptic solutions for these equations. Ali et al. [2] proposed and analyzed a novel spectral scheme to get the numerical solutions of the two-dimensional time-fractional diffusion equation.

This study aims to obtain numerical solutions of the mCH (4) and mDP (5) equations with initial and boundary conditions as follows:

$$\begin{gathered} U_t - U_{xxt} + 3U^2U_x - 2U_xU_{xx} - UU_{xxx} = 0, \quad x \in (a,b),\ t \geq 0, \\ U(x,0) = -2\sec h^2(\frac{x}{2}),\ U(a,t) = f_1(t),\ U(b,t) = f_2(t), \\ U'(a,t) = f_3(t),\ U'(b,t) = f_4(t),\ U''(a,t) = f_5(t),\ U''(b,t) = f_6(t) \end{gathered} \tag{4}$$

and

$$\begin{gathered} U_t - U_{xxt} + 4U^2U_x - 3U_xU_{xx} - UU_{xxx} = 0, \quad x \in (a,b),\ t \geq 0, \\ U(x,0) = -\frac{15}{8}\sec h^2(\frac{x}{2}),\ U(a,t) = g_1(t),\ U(b,t) = g_2(t), \\ U'(a,t) = g_3(t),\ U'(b,t) = g_4(t),\ U''(a,t) = g_5(t),\ U''(b,t) = g_6(t). \end{gathered} \tag{5}$$

This article is planned as follows: in Section 2, to obtain numerical solutions of the b-equation which contains very strong nonlinear terms with higher order derivatives, a powerful computationally hybrid technique utilizing finite element and finite difference methods together has been presented. Also, in this section, the stability of the scheme is examined by the von Neumann method so that the approximate solutions obtained from the numerical scheme resulting in the algebraic equation system remain close to the analytical solutions of the b-equation with acceptable accuracy, and it is shown that the scheme is unconditionally stable. In Section 3, numerical schemes obtained by applying the presented method to both mCH and mDP equations subject to initial and boundary conditions are given. In addition, to show the accuracy and

reliability of the numerical schemes, some numerical results calculated using the same parameters are compared with themselves and also those obtained by other researchers. In Section 4 which is the last section, a brief conclusion is given and a suggestion for future work is also made.

2. Trigonometric Quintic B-spline Collocation Method

Since it is impossible to implement a numerical method on all $x \in R$ and semi-infinite $t \in R^+$, the solution region of the considered problems below for numerical simulations is taken as $a \le x \le b$ and $0 \le t \le T$. The principal idea of a finite element formulation using for obtaining an approximate solution of a physical problem is to result in algebraic equation systems rather than solving differential equations [9, 13]. For this purpose, let x_m be a uniform finite fragmentation of the solution region $[a,b]$, and $a = x_0 < x_1 < \ldots < x_N = b$, where $m = 0, 1, \ldots, N$. Taking $h = x_{m+1} - x_m$, $T_m(x)$, $m = -2(1)N + 2$, quintic trigonometric B-spline functions on the range $[a,b]$ in terms of nodes x_m as

$$T_m(x) = \frac{1}{\theta}\begin{cases} \tau^5(x_{m-3}) \ , & [x_{m-3}, x_{m-2}] \\ \tau^4(x_{m-3})\phi(x_{m-1}) + \tau^3(x_{m-3})\phi(x_m)\tau(x_{m-2}) + \\ \tau^2(x_{m-3})\phi(x_{m+1})\tau^2(x_{m-2}) + & [x_{m-2}, x_{m-1}] \\ \tau(x_{m-3})\phi(x_{m+2})\tau^3(x_{m-2}) + \phi(x_{m+3})\tau^4(x_{m-2}), \\ \tau^3(x_{m-3})\phi^2(x_m) + \tau^2(x_{m-3})\phi(x_{m+1})\tau(x_{m-2})\phi(x_m) \\ +\tau^2(x_{m-3})\phi^2(x_{m+1})\tau(x_{m-1}) + \tau(x_{m-3})\phi(x_{m+2})\tau^2(x_{m-2})\phi(x_m) + \\ \tau(x_{m-3})\phi(x_{m+2})\tau(x_{m-2})\phi(x_{m+1})\tau(x_{m-1}) + & [x_{m-1}, x_m] \\ \tau(x_{m-3})\phi^2(x_{m+2})\tau^2(x_{m-1}) + \\ \phi(x_{m+3})\tau^3(x_{m-2})\phi(x_m) + \phi(x_{m+3})\tau^2(x_{m-2})\phi(x_{m+1})\tau(x_{m-1}) + \\ \phi(x_{m+3})\tau(x_{m-2})\phi(x_{m+2})\tau^2(x_{m-1}) + \phi^2(x_{m+3})\tau^3(x_{m-1}), \\ \tau^2(x_{m-3})\phi^3(x_{m+1}) + \tau(x_{m-3})\phi(x_{m+2})\tau(x_{m-2})\phi^2(x_{m+1}) + \\ \tau(x_{m-3})\phi^2(x_{m+2})\tau(x_{m-1})\phi(x_{m+1}) + \tau(x_{m-3})\phi^3(x_{m+2})\tau(x_m) + \\ \phi(x_{m+3})\tau^2(x_{m-2})\phi^2(x_{m+1}) + & [x_m, x_{m+1}] \\ \phi(x_{m+3})\tau(x_{m-2})\phi(x_{m+2})\tau(x_{m-1})\phi(x_{m+1}) + \\ \phi(x_{m+3})\tau(x_{m-2})\phi^2(x_{m+2})\tau(x_m) + \phi^2(x_{m+3})\tau^2(x_{m-1})\phi(x_{m+1}) + \\ \phi^2(x_{m+3})\tau(x_{m-1})\phi(x_{m+2})\tau(x_m) + \phi^3(x_{m+3})\tau^2(x_m), \\ \tau(x_{m-3})\phi^4(x_{m+2}) + \phi(x_{m+3})\tau(x_{m-2})\phi^3(x_{m+2}) + \\ \phi^2(x_{m+3})\tau(x_{m-1})\phi^2(x_{m+2}) + & [x_{m+1}, x_{m+2}] \\ \phi^3(x_{m+3})\tau(x_m)\phi(x_{m+2}) + \phi^4(x_{m+3})\tau(x_{m+1}), \\ \phi^5(x_{m+3}), & [x_{m+2}, x_{m+3}] \\ 0, & \text{otherwise} \end{cases} \tag{6}$$

where $\theta = \sin(\frac{h}{2})\sin(h)\sin(\frac{3h}{2})\sin(2h)\sin(\frac{5h}{2})$, $\tau(x_m) = \sin(\frac{x-x_m}{2})$ and $\phi(x_m) = \sin(\frac{x_m-x}{2})$. It is clear that the set $\{T_{-2}(x), T_{-1}(x), \ldots, T_{N+1}(x), T_{N+2}(x)\}$ forms a base on the interval $[a,b]$ [7, 15]. A typical element $[x_m, x_{m+1}]$ transforms into the interval $[0,1]$ by using $h\xi = x - x_m$. Hence each $[x_m, x_{m+1}]$ element is covered by six trigonometric quntıc B-splines such as $T_{m-2}(x)$, $T_{m-1}(x)$, $T_m(x)$, $T_{m+1}(x)$, $T_{m+2}(x)$, $T_{m+3}(x)$. Thus, the approximate solution via trigonometric

quintic B-spline functions on the element $[x_m, x_{m+1}]$ can be written as

$$U(x,t) \approx U_N(x,t) = \sum_{i=m-2}^{m+3} T_i(x)\delta_i(t).$$

Using (6), the nodal values of $U_N(x,t)$ and its third order derivatives at the nodes x_m are obtained as

$$\begin{aligned} U_N(x_m,t) &= U_m = a_1\delta_{m-2} + a_2\delta_{m-1} + a_3\delta_m + a_2\delta_{m+1} + a_1\delta_{m+2}, \\ U_m^{'} &= -a_4\delta_{m-2} - a_5\delta_{m-1} + a_5\delta_{m+1} + a_4\delta_{m+2}, \\ U_m^{''} &= a_6\delta_{m-2} + a_7\delta_{m-1} + a_8\delta_m + a_7\delta_{m+1} + a_6\delta_{m+2}, \\ U_m^{'''} &= -a_9\delta_{m-2} + a_{10}\delta_{m-1} - a_{10}\delta_{m+1} + a_9\delta_{m+2}, \end{aligned} \tag{7}$$

where

$$a_1 = \sin^5(\frac{h}{2})/\theta,\ a_2 = \sin^4(\frac{h}{2})\sin(h)(8\cos(h)+5)/\theta,\ a_3 = 2\sin^5(\frac{h}{2})(6\cos(2h)+16\cos(h)+11)/\theta,$$

$$a_4 = 5\sin^3(\frac{h}{2})\sin(h)/4\theta,\ a_5 = 5\sin^4(\frac{h}{2})\cos^2(\frac{h}{2})(4\cos(h)+1)/\theta,\ a_6 = 5\sin^3(\frac{h}{2})(5\cos(h)+3)/8\theta,$$

$$a_7 = 5\sin^3(\frac{h}{2})\cos(\frac{h}{2})(4\cos(2h)+\cos(h)+3)/4\theta,\ a_8 = -5\sin^3(\frac{h}{2})(\cos(3h)+6\cos(2h)+10\cos(h)+7)/4\theta,$$

$$a_9 = 5\sin^2(\frac{h}{2})\cos(\frac{h}{2})(25\cos(h)-1)/16\theta,\ a_{10} = -5\sin^2(h)(2\cos(2h)-27\cos(h)+1)/32\theta.$$

If the expressions given in (7) are used in Equation (3), an ordinary differential equation system is obtained as follows:

$$\begin{aligned} &a_1\overset{\circ}{\delta}_{m-2} + a_2\overset{\circ}{\delta}_{m-1} + a_3\overset{\circ}{\delta}_m + a_2\overset{\circ}{\delta}_{m+1} + a_1\overset{\circ}{\delta}_{m+2} \\ &-(a_6\overset{\circ}{\delta}_{m-2} + a_7\overset{\circ}{\delta}_{m-1} + a_8\overset{\circ}{\delta}_m + a_7\overset{\circ}{\delta}_{m+1} + a_6\overset{\circ}{\delta}_{m+2}) \\ &+z_m^2(b+1)\left(-a_4\delta_{m-2} - a_5\delta_{m-1} + a_5\delta_{m+1} + a_4\delta_{m+2}\right) \\ &-bt_m\left(a_6\delta_{m-2} + a_7\delta_{m-1} + a_8\delta_m + a_7\delta_{m+1} + a_6\delta_{m+2}\right) \\ &-z_m\left(-a_9\delta_{m-2} + a_{10}\delta_{m-1} - a_{10}\delta_{m+1} + a_9\delta_{m+2}\right) = 0, \end{aligned} \tag{8}$$

where the symbol "$\circ$"is the derivative concerning time and

$$\begin{aligned} z_m &= \delta_{m-2} + 26\delta_{m-1} + 66\delta_m + 26\delta_{m+1} + \delta_{m+2}, \\ d_m &= \frac{5}{h}(-\delta_{m-2} - 10\delta_{m-1} + 10\delta_{m+1} + \delta_{m+2}). \end{aligned}$$

Instead of the parameters δ_m and $\overset{\circ}{\delta}_m$, $\frac{\delta_m^{n+1}+\delta_m^n}{2}$ Crank-Nicolson and $\frac{\delta_m^{n+1}-\delta_m^n}{\Delta t}$ forward finite difference approaches are written in Equation (8) respectively, a recurrence relation is obtained between time steps n and $(n+1)$ as

$$\begin{aligned}&\kappa_1\delta_{m-2}^{n+1}+\kappa_2\delta_{m-1}^{n+1}+\kappa_3\delta_m^{n+1}+\kappa_4\delta_{m+1}^{n+1}+\kappa_5\delta_{m+2}^{n+1}\\&=\kappa_6\delta_{m-2}^{n}+\kappa_7\delta_{m-1}^{n}+\kappa_8\delta_m^{n}+\kappa_9\delta_{m+1}^{n}+\kappa_{10}\delta_{m+2}^{n},\end{aligned}\tag{9}$$

where

$$\kappa_1=a_1-a_6-\frac{a_4(b+1)z_m^2\Delta t}{2}-\frac{ba_6d_m\Delta t}{2}+\frac{a_9z_m\Delta t}{2},$$

$$\kappa_2=a_2-a_7-\frac{a_5(b+1)z_m^2\Delta t}{2}-\frac{ba_7d_m\Delta t}{2}-\frac{a_{10}z_m\Delta t}{2},$$

$$\kappa_3=a_3-a_8-\frac{ba_8d_m\Delta t}{2},\ \kappa_4=a_2-a_7+\frac{a_5(b+1)z_m^2\Delta t}{2}-\frac{ba_7d_m\Delta t}{2}+\frac{a_{10}z_m\Delta t}{2},$$

$$\kappa_5=a_1-a_6+\frac{a_4(b+1)z_m^2\Delta t}{2}-\frac{ba_6d_m\Delta t}{2}-\frac{a_9z_m\Delta t}{2},$$

$$\kappa_6=a_1-a_6+\frac{a_4(b+1)z_m^2\Delta t}{2}+\frac{ba_6d_m\Delta t}{2}-\frac{a_9z_m\Delta t}{2},$$

$$\kappa_7=a_2-a_7+\frac{a_5(b+1)z_m^2\Delta t}{2}+\frac{ba_7d_m\Delta t}{2}+\frac{a_{10}z_m\Delta t}{2},\ \kappa_8=a_3-a_8+\frac{ba_8d_m\Delta t}{2},$$

$$\kappa_9=a_2-a_7-\frac{a_5(b+1)z_m^2\Delta t}{2}+\frac{ba_7d_m\Delta t}{2}-\frac{a_{10}z_m\Delta t}{2},$$

$$\kappa_{10}=a_1-a_6-\frac{a_4(b+1)z_m^2\Delta t}{2}+\frac{ba_6d_m\Delta t}{2}+\frac{a_9z_m\Delta t}{2}.$$

The algebraic equation system (9) contains $(N+1)$ equations and $(N+5)$ time-dependent parameters $\delta_m(t)$, $m=0(1)N$. To have a unique solution for this system, the parameters δ_{-2}, δ_{-1}, δ_{N+1} and δ_{N+2} must be eliminated with the help of boundary conditions. If the approaches U_m and U_m' are used to transform the system (9) into an $(N+1)\times(N+1)$ pentadiagonal system, the following relations are obtained for the parameters δ_{-2}, δ_{-1}, δ_{N+1}, and δ_{N+2}

$$\begin{aligned}\delta_{-2}&=m_1\delta_0+m_2\delta_1+m_3\delta_2+\lambda_1,\ \ \delta_{-1}=m_4\delta_0+m_5\delta_1+m_6\delta_2+\lambda_2\ ,\\ \delta_{N+1}&=m_6\delta_{N-2}+m_5\delta_{N-1}+m_4\delta_N+\lambda_3,\ \delta_{N+2}=m_3\delta_{N-2}+m_2\delta_{N-1}+m_1\delta_N+\lambda_4,\end{aligned}$$

where

$$
\begin{aligned}
m_1 &= \frac{a_3a_5}{a_2a_4-a_1a_5},\ m_2=\frac{2a_2a_5}{a_2a_4-a_1a_5},\ m_3=\frac{a_1a_5+a_2a_4}{a_2a_4-a_1a_5},\\
m_4 &= \frac{a_3a_4}{a_1a_5-a_2a_4},\ m_5=\frac{a_2a_4+a_1a_5}{a_1a_5-a_2a_4},\ m_6=\frac{2a_1a_4}{a_1a_5-a_2a_4},\\
\lambda_1 &= \frac{a_2U'(a,t)+a_5U(a,t)}{a_1a_5-a_2a_4},\ \lambda_2=\frac{a_4U(a,t)+a_1U'(a,t)}{a_2a_4-a_1a_5},\\
\lambda_3 &= \frac{a_1U'(b,t)-a_4U(b,t)}{a_1a_5-a_2a_4},\ \lambda_4=\frac{a_2U'(b,t)-a_5U(b,t)}{a_2a_4-a_1a_5}.
\end{aligned}
$$

To start the solution of the system (9), it is necessary to find the initial vector δ_m^0. For this purpose, similar to the above, after finding relations for δ_{-2}, δ_{-1}, δ_{N+1}, and δ_{N+2} with the help of $U_m^{'}$ and $U_m^{''}$, the initial vector is generated from the solution of the below matrix system.

$$
\begin{bmatrix}
\alpha_1 & \alpha_2 & \alpha_3 & & & & \\
\alpha_4 & \alpha_5 & \alpha_6 & a_1 & & & \\
a_1 & a_2 & a_3 & a_2 & a_1 & & \\
 & & & \ddots & & & \\
 & & a_1 & a_2 & a_3 & a_2 & a_1 \\
 & & & a_1 & \alpha_6 & \alpha_5 & \alpha_4 \\
 & & & & \alpha_3 & \alpha_2 & \alpha_1
\end{bmatrix}
\begin{bmatrix} \delta_0^0 \\ \delta_1^0 \\ \delta_2^0 \\ \vdots \\ \delta_{N-2}^0 \\ \delta_{N-1}^0 \\ \delta_N^0 \end{bmatrix}
=
\begin{bmatrix} U_0 \\ U_1 \\ U_2 \\ \vdots \\ U_{N-2} \\ U_{N-1} \\ U_N \end{bmatrix}
+
\begin{bmatrix} \gamma_1 \\ \gamma_2 \\ 0 \\ \vdots \\ 0 \\ \gamma_3 \\ \gamma_4 \end{bmatrix},
$$

where

$$
\alpha_1=a_1\beta_4+a_2\beta_1+a_3,\ \alpha_2=a_1\beta_5+a_2\beta_2+a_2,\ \alpha_3=a_1\beta_6+a_2\beta_3+a_1,
$$

$$
\alpha_4=a_1\beta_1+a_2,\ \alpha_5=a_1\beta_2+a_3,\ \alpha_6=a_1\beta_3+a_2,\ \beta_1=\frac{a_4a_8}{a_5a_6-a_4a_7},
$$

$$
\beta_2=\frac{a_4a_7+a_5a_6}{a_5a_6-a_4a_7},\ \beta_3=\frac{2a_4a_6}{a_5a_6-a_4a_7},\ \beta_4=\frac{a_5a_8}{a_4a_7-a_5a_6},\ \beta_5=\frac{2a_5a_7}{a_4a_7-a_5a_6},\ \beta_6=\frac{a_5a_6+a_4a_7}{a_4a_7-a_5a_6},
$$

$$
\gamma_1=\frac{(a_1a_5-a_2a_4)U^{''}(a,0)+(a_1a_7-a_2a_6)U^{'}(a,0)}{a_5a_6-a_4a_7},\ \gamma_2=\frac{a_1a_4U^{''}(a,0)+a_1a_6U^{'}(a,0)}{a_4a_7-a_5a_6},
$$

$$
\gamma_3=\frac{a_1a_6U^{'}(b,0)-a_1a_4U^{''}(b,0)}{a_5a_6-a_4a_7},\ \gamma_4=\frac{(a_2a_6-a_1a_7)U^{'}(b,0)+(a_1a_5-a_2a_4)U^{''}(b,0)}{a_5a_6-a_4a_7}.
$$

2.1. Stability Analysis

To investigate the stability analysis of the system (9), the Fourier series method of von Neumann [14] is used. In this method, $\delta_m^n=\xi^n e^{i\beta mh}$ is taken, where $i=\sqrt{-1}$, β is the mode number, ξ is the amplification factor, and h is the space step. Since this method is valid for linear schemes, the z_m and d_m constants are taken to be zero. If $\delta_m^n=\xi^n e^{i\beta mh}$ is written in the system (9) and if

necessary operations are performed, the following expressions are obtained:

$$\frac{\xi(t^{n+1})}{\xi(t^n)} = \frac{\kappa_6 e^{-2i\beta h} + \kappa_7 e^{-i\beta h} + \kappa_8 + \kappa_9 e^{i\beta h} + \kappa_{10} e^{2i\beta h}}{\kappa_1 e^{-2i\beta h} + \kappa_2 e^{-i\beta h} + \kappa_3 + \kappa_4 e^{i\beta h} + \kappa_5 e^{2i\beta h}}$$

or

$$\begin{aligned}\frac{\xi(t^{n+1})}{\xi(t^n)} &= \frac{[(\kappa_6+\kappa_{10})\cos(2\beta h)+(\kappa_7+\kappa_9)\cos(\beta h)+\kappa_8]+i[(\kappa_{10}-\kappa_6)\sin(2\beta h)+(\kappa_9-\kappa_7)\sin(\beta h)]}{[(\kappa_1+\kappa_5)\cos(2\beta h)+(\kappa_2+\kappa_4)\cos(\beta h)+\kappa_3]+i[(\kappa_5-\kappa_1)\sin(2\beta h)+(\kappa_4-\kappa_2)\sin(\beta h)]} \\ &= \frac{P+iQ}{R+iS},\end{aligned}$$

where

$$\begin{aligned}P &= [(\kappa_6+\kappa_{10})\cos(2\beta h)+(\kappa_7+\kappa_9)\cos(\beta h)+\kappa_8], \\ Q &= [(\kappa_{10}-\kappa_6)\sin(2\beta h)+(\kappa_9-\kappa_7)\sin(\beta h)], \\ R &= [(\kappa_1+\kappa_5)\cos(2\beta h)+(\kappa_2+\kappa_4)\cos(\beta h)+\kappa_3], \\ S &= [(\kappa_5-\kappa_1)\sin(2\beta h)+(\kappa_4-\kappa_2)\sin(\beta h)].\end{aligned}$$

For the stability of the method, the condition $\left|\frac{\xi(t^{n+1})}{\xi(t^n)}\right| \le 1$ must be provided. Namely, the inequality $|P^2|+|Q^2| \le |R^2|+|S^2|$ must be ensured. Thus, the following expression is obtained:

$$|P^2|+|Q^2|-|R^2|-|S^2| \le 0.$$

Since $|P^2|+|Q^2|-|R^2|-|S^2| \le 0$, the method is unconditionally stable. Besides, it should still be taken into account that the solutions are not distorted when choosing h and Δt.

3. Numerical Applications

In this section, two test problems have been considered for the numerical simulations. To confirm the accuracy and efficiency of the proposed method, we have calculated L_2, L_∞ error norms, and absolute error (AE) that measure the difference between exact (u) and numerical (u_N) solutions as follows:

$$L_2 = \sqrt{h\sum_{j=0}^{N} |U(x_j,t)-U_N(x_j,t)|^2},\ L_\infty = \max_{0\le j\le N} |U(x_j,t)-U_N(x_j,t)|,\ \mathrm{AE} = |U(x_j,t)-U_N(x_j,t)|.$$

Table 1: The error norms L_2 and L_∞ for $h = 0.1$ and $\Delta t = 0.01,\ 0.001$ over $-40 \le x \le 40$ and the maximum amplitude and positions of the soliton waves for mCH

Δt	t	L_2	L_∞	x	Present	Exact
0.01	0	0	0	0.00	−2.0000000000	−2.0000000000
	2	0.257512E-3	0.137435E-3	4.00	−1.9999984012	−2.0000000000
	4	0.507308E-3	0.268631E-3	8.00	−1.9999981491	−2.0000000000
	6	0.755920E-3	0.399642E-3	12.00	−1.9999980667	−2.0000000000
	8	1.004526E-3	0.530661E-3	16.00	−1.9999979597	−2.0000000000
	10	1.253169E-3	0.661694E-3	20.00	−1.9999978238	−2.0000000000
0.001	2	0.143124E-5	0.568181E-6	4.00	−1.9999997739	−2.0000000000
	4	0.204605E-5	0.845279E-6	8.00	−1.9999997094	−2.0000000000
	6	0.269423E-5	0.133650E-5	12.00	−1.9999997070	−2.0000000000
	8	0.356980E-5	0.189265E-5	16.00	−1.9999997069	−2.0000000000
	10	0.456604E-5	0.247223E-5	20.00	−1.9999997069	−2.0000000000

3.1. Soliton Solutions of mCH Equation

As a first application, consider the modified Camassa-Holm (4) equation with initial and boundary conditions as follows:

$$U_t - u_{xxt} + 3U^2U_x - 2U_xU_{xx} - UU_{xxx} = 0, \quad x \in (a,b),\ t \ge 0,$$

$$U(x,0) = -2\sec h^2(\frac{x}{2}),\ U(a,t) = f_1(t),\ U(b,t) = f_2(t),$$

$$U'(a,t) = f_3(t),\ U'(b,t) = f_4(t),\ U''(a,t) = f_5(t),\ U''(b,t) = f_6(t).$$

The numerical results obtained by solving the mCH (4) equation are presented in Table 1. As shown from the Table 2, as Δt gets smaller, the error norms L_2 and L_∞ also decrease significantly. The wave's amplitude at $t = 0$ is calculated as -2 at $x = 0$ and -1.9999997069 at $x = 20$ at $t = 10$, and this change is 2.931×10^{-7}. It is seen that the numerical results given in different locations and times in the Table 2 are very close to the exact solution. In the Table 3, some nodal values have been compared to the analytic solution. In addition to comparing the absolute errors with Ref. [16], the error norms L_2 and L_∞ are also given. The numerical results given by the current method in the Table 3 converge to a better exact solution than those given in Ref. [16]. In Figure 1, the physical behavior of the numerical and analytic solution (*upper*) and the absolute error graphs (*bottom*) at different times are given. It can be seen from Figure 1 that the waves are moving to the right, keeping their speed and height almost perfect.

Table 2: Some nodal values of $U(x,t)$ for $h = 0.1$ and $\Delta t = 0.001$ over $-15 \le x \le 15$ of mCH

t	x	Numeric	Analytic	t	x	Numeric	Analytic
	−12	−0.0000444755	−0.0000444756		−12	−0.0000364134	−0.0000364136
	−10	−0.0003286090	−0.0003286094		−10	−0.0002690455	−0.0002690467
	−9	−0.0008931260	−0.0008931270		−9	−0.0007312574	−0.0007312601
	−8	−0.0024268374	−0.0024268396		−8	−0.0019871407	−0.0019871468
0.05	−6	−0.0178627158	−0.0178627244	0.15	−6	−0.0146366096	−0.0146366342
	6	−0.0217959864	−0.0217959772		6	−0.0265895200	−0.0265894909
	8	−0.0029637527	−0.0029637503		8	−0.0036193465	−0.0036193389
	9	−0.0010908149	−0.0010908138		9	−0.0013322461	−0.0013322426
	10	−0.0004013577	−0.0004013572		10	−0.0004902094	−0.0004902079
	12	−0.0000543226	−0.0000543225		12	−0.0000663497	−0.0000663495
	−12	−0.0000402431	−0.0000402432		−12	−0.0000329482	−0.0000329484
	−10	−0.0002973396	−0.0002973404		−10	−0.0002434435	−0.0002434450
	−9	−0.0008081500	−0.0008081519		−9	−0.0006616795	−0.0006616830
	−8	−0.0021960179	−0.0021960221		−8	−0.0017981220	−0.0017981298
0.10	−6	−0.0161697309	−0.0161697477	0.20	−6	−0.0132483638	−0.0132483957
	6	−0.0240744628	−0.0240744439		6	−0.0293653701	−0.0293653302
	8	−0.0032752003	−0.0032751954		8	−0.0039996179	−0.0039996072
	9	−0.0012055034	−0.0012055012		9	−0.0014723091	−0.0014723042
	10	−0.0004435646	−0.0004435636		10	−0.0005417587	−0.0005417565
	12	−0.0000600357	−0.0000600356		12	−0.0000733277	−0.0000733274

Table 3: Some nodal values of $U(x,t)$ and comparison of absolute error with Ref. [16] for $h = 0.1$ and $\Delta t = 0.001$ over $-15 \le x \le 15$ of mCH

t	x	Numeric	Analytic	Present (AE)	[16] (AE)
	6	−0.0217959864	−0.0217959772	0.918E−8	3.349E−04
	8	−0.0029637527	−0.0029637503	0.236E−8	4.359E−05
0.05	9	−0.0010908149	−0.0010908138	0.108E−8	1.596E−05
	10	−0.0004013577	−0.0004013572	0.475E−9	5.860E−06
	12	−0.0000543226	−0.0000543225	0.852E−10	7.900E−07
	6	−0.0240744628	−0.0240744439	0.189E−7	8.847E−04
	8	−0.0032752003	−0.0032751954	0.491E−8	1.159E−04
0.10	9	−0.0012055034	−0.0012055012	0.225E−8	4.248E−05
	10	−0.0004435646	−0.0004435636	0.993E−9	1.560E−05
	12	−0.0000600357	−0.0000600356	0.178E−9	2.100E−06
	8	−0.0036193465	−0.0036193389	0.766E−8	2.238E−04
0.15	9	−0.0013322461	−0.0013322426	0.352E−8	8.208E−05
	10	−0.0004902094	−0.0004902079	0.155E−8	3.014E−05
	8	−0.0039996179	−0.0039996072	0.106E−7	3.765E−04
0.20	9	−0.0014723091	−0.0014723042	0.490E−8	1.381E−04
	10	−0.0005417587	−0.0005417565	0.217E−8	5.073E−05

	$t = 0.05$	$t = 0.1$	$t = 0.15$	$t = 0.20$
$L_2 \times 10^6$	0.045859	0.091547	0.136939	0.181932
$L_\infty \times 10^6$	0.202146	0.401670	0.590314	0.768287

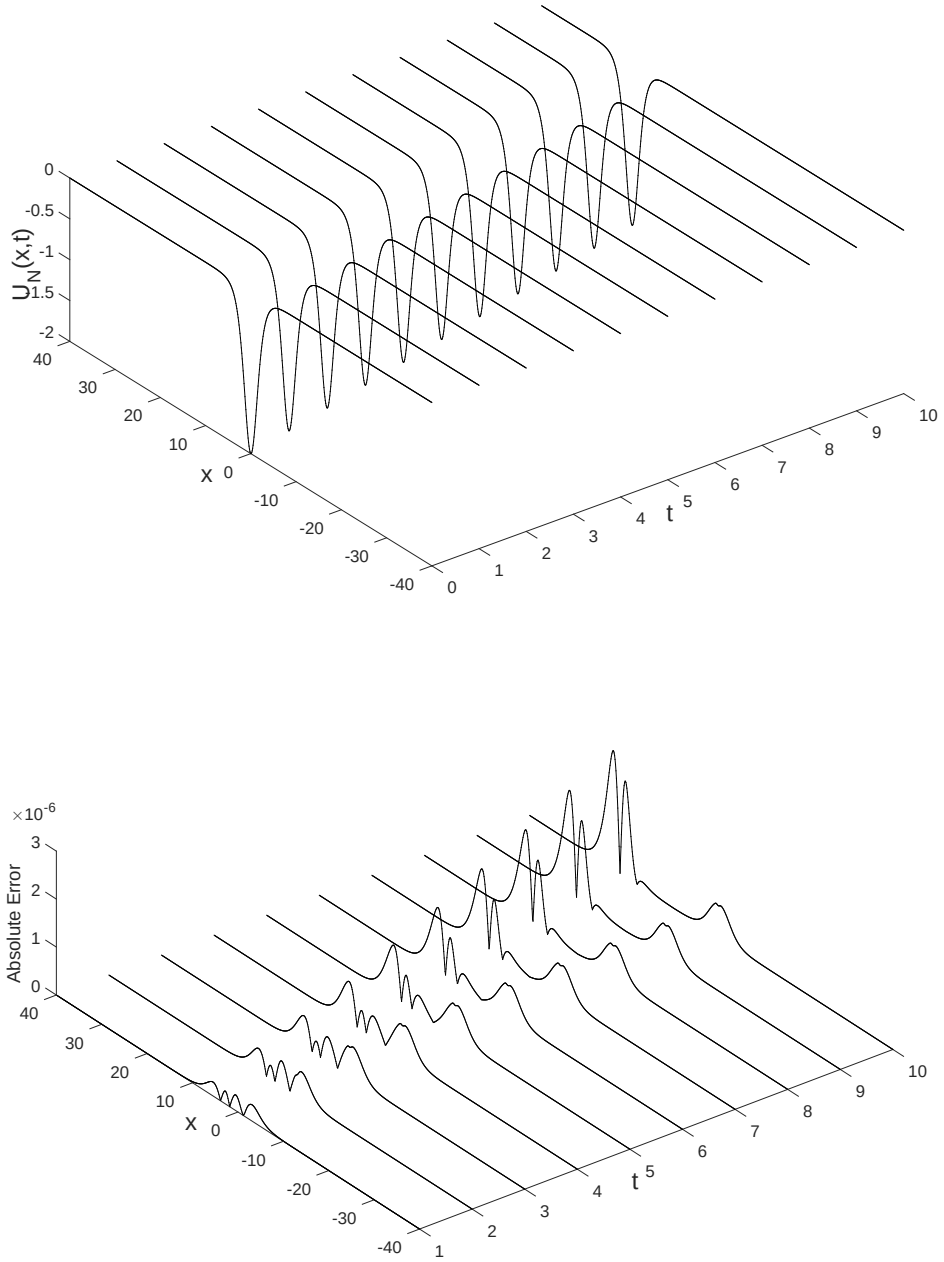

Figure 1: Soliton wave progression (*upper*) and absolute error (*bottom*) of the mCH equation for $h = 0.1,\ \Delta t = 0.001$

Table 4: The error norms L_2 and L_∞ for $h = 0.1$ and $\Delta t = 0.01,\ 0.001$ over $-40 \le x \le 40$ and the maximum amplitude and positions of the waves for mDP

Δt	t	L_2	L_∞	x	Present	Exact
0.01	0	0	0	0.00	−1.8750000000	−1.8750000000
	2	0.502693E-3	0.269075E-3	5.00	−1.8749969077	−1.8750000000
	4	0.987224E-3	0.524039E-3	10.00	−1.8749966431	−1.8750000000
	6	1.470814E-3	0.778917E-3	15.00	−1.8749963319	−1.8750000000
	8	1.954544E-3	1.033844E-3	20.00	−1.8749959041	−1.8750000000
	10	2.438395E-3	1.288820E-3	25.00	−1.8749953600	−1.8750000000
0.001	2	0.284646E-5	0.159639E-5	5.00	−1.8749997931	−1.8750000000
	4	0.372017E-5	0.199237E-5	10.00	−1.8749997716	−1.8750000000
	6	0.426197E-5	0.230974E-5	15.00	−1.8749997713	−1.8750000000
	8	0.481290E-5	0.262623E-5	20.00	−1.8749997709	−1.8750000000
	10	0.537967E-5	0.297078E-5	25.00	−1.8749997512	−1.8750000000

3.2. Soliton Solutions of mDP Equation

As a second and last application, consider the modified Degasperis-Procesi (5) equation with initial and boundary conditions as follows:

$$U_t - U_{xxt} + 4U^2U_x - 3U_xU_{xx} - uu_{xxx} = 0,\quad x \in (a,b),\ t \ge 0,$$

$$U(x,0) = -\frac{15}{8}\sec h^2(\frac{x}{2}),\ U(a,t) = g_1(t),\ U(b,t) = g_2(t),$$

$$U'(a,t) = g_3(t),\ U'(b,t) = g_4(t),\ U''(a,t) = g_5(t),\ U''(b,t) = g_6(t).$$

The numerical results obtained by solving the mDP (5) equation are given in the Table 4. As shown from the table, the error norms L_2 and L_∞ decrease significantly as Δt gets smaller. Also, the wave's amplitude at $t = 0$ is -1.875 at $x = 0$ and -1.8749997512 at $x = 25$ at $t = 10$, and this change is 2.488×10^{-7}. It is seen that the numerical results given in different locations and times in the Table 5 are quite close to the analytic solution. In the Table 6, some nodal values are compared with the exact solution as well as Ref. [16] a comparison of with absolute errors and L_2, L_∞ error norms are also given. The numerical results obtained with the proposed method converge better than those given in Ref. [16]. In Figure 2, the physical behavior of the numerical and exact solution (*upper*) and the absolute error graphs (*bottom*) at different times are given. It can be seen from Figure 2 that the waves move to the right, keeping their speed and height almost admirably.

4. Conclusions

In this study, soliton wave solutions of the modified Camassa-Holm (mCH) and Degasperis-Process (mDP) equations were obtained by the trigonometric quintic B-spline collocation finite element

Table 5: Some nodal values of $U(x,t)$ for $h = 0.1$ and $\Delta t = 0.001$ over $-15 \le x \le 15$ of mDP

t	x	Numeric	Analytic	t	x	Numeric	Analytic
	−12	−0.0000406663	−0.0000406664		−12	−0.0000316709	−0.0000316711
	−10	−0.0003004651	−0.0003004657		−10	−0.0002340057	−0.0002340070
	−9	−0.0008166367	−0.0008166379		−9	−0.0006360257	−0.0006360289
	−8	−0.0022190189	−0.0022190214		−8	−0.0017283949	−0.0017284019
0.05	−6	−0.0163346314	−0.0163346415	0.15	−6	−0.0127336964	−0.0127337247
	6	−0.0209481240	−0.0209481133		6	−0.0268551982	−0.0268551645
	8	−0.0028488037	−0.0028488009		8	−0.0036571525	−0.0036571434
	9	−0.0010485202	−0.0010485189		9	−0.0013462223	−0.0013462180
	10	−0.0003857973	−0.0003857968		10	−0.0004953602	−0.0004953584
	12	−0.0000522167	−0.0000522166		12	−0.0000670475	−0.0000670471
	−12	−0.0000358879	−0.0000358880		−12	−0.0000279494	−0.0000279497
	−10	−0.0002651615	−0.0002651625		−10	−0.0002065102	−0.0002065120
	−9	−0.0007206966	−0.0007206988		−9	−0.0005613007	−0.0005613047
	−8	−0.0019584109	−0.0019584157		−8	−0.0015253831	−0.0015253920
0.10	−6	−0.0144226482	−0.0144226677	0.20	−6	−0.0112419288	−0.0112419653
	6	−0.0237196488	−0.0237196269		6	−0.0304018338	−0.0304017877
	8	−0.0032277936	−0.0032277878		8	−0.0041435608	−0.0041435480
	9	−0.0011880860	−0.0011880834		9	−0.0015253979	−0.0015253920
	10	−0.0004371602	−0.0004371590		10	−0.0005613073	−0.0005613047
	12	−0.0000591692	−0.0000591690		12	−0.0000759746	−0.0000759742

Table 6: Some nodal values of $U(x,t)$ and comparison of absolute error with Ref. [16] for $h = 0.1$ and $\Delta t = 0.001$ over $-15 \le x \le 15$ of mDP

t	x	Numeric	Analytic	Present (AE)	[16] (AE)
	6	−0.0209481240	−0.0209481133	0.106E−7	4.490E−04
	8	−0.0028488037	−0.0028488009	0.277E−8	6.312E−05
0.05	9	−0.0010485202	−0.0010485189	0.127E−8	2.332E−05
	10	−0.0003857973	−0.0003857968	0.560E−9	8.590E−06
	12	−0.0000522167	−0.0000522166	0.101E−9	1.160E−06
	6	−0.0237196488	−0.0237196269	0.219E−7	9.037E−04
	8	−0.0032277936	−0.0032277878	0.581E−8	1.276E−04
0.10	9	−0.0011880860	−0.0011880834	0.267E−8	4.720E−05
	10	−0.0004371602	−0.0004371590	0.118E−8	1.740E−05
	12	−0.0000591692	−0.0000591690	0.212E−9	2.350E−06
	8	−0.0036571525	−0.0036571434	0.912E−8	1.932E−04
0.15	9	−0.0013462223	−0.0013462180	0.421E−8	1.461E−05
	10	−0.0004953602	−0.0004953584	0.186E−8	2.635E−05
	8	−0.0041435608	−0.0041435480	0.127E−7	2.585E−04
0.20	9	−0.0015253979	−0.0015253920	0.590E−8	9.568E−05
	10	−0.0005613073	−0.0005613047	0.285E−8	3.529E−05

	$t = 0.05$	$t = 0.1$	$t = 0.15$	$t = 0.20$
$L_2 \times 10^6$	0.094519	0.188815	0.282694	0.375984
$L_\infty \times 10^6$	0.054802	0.109182	0.162013	0.212648

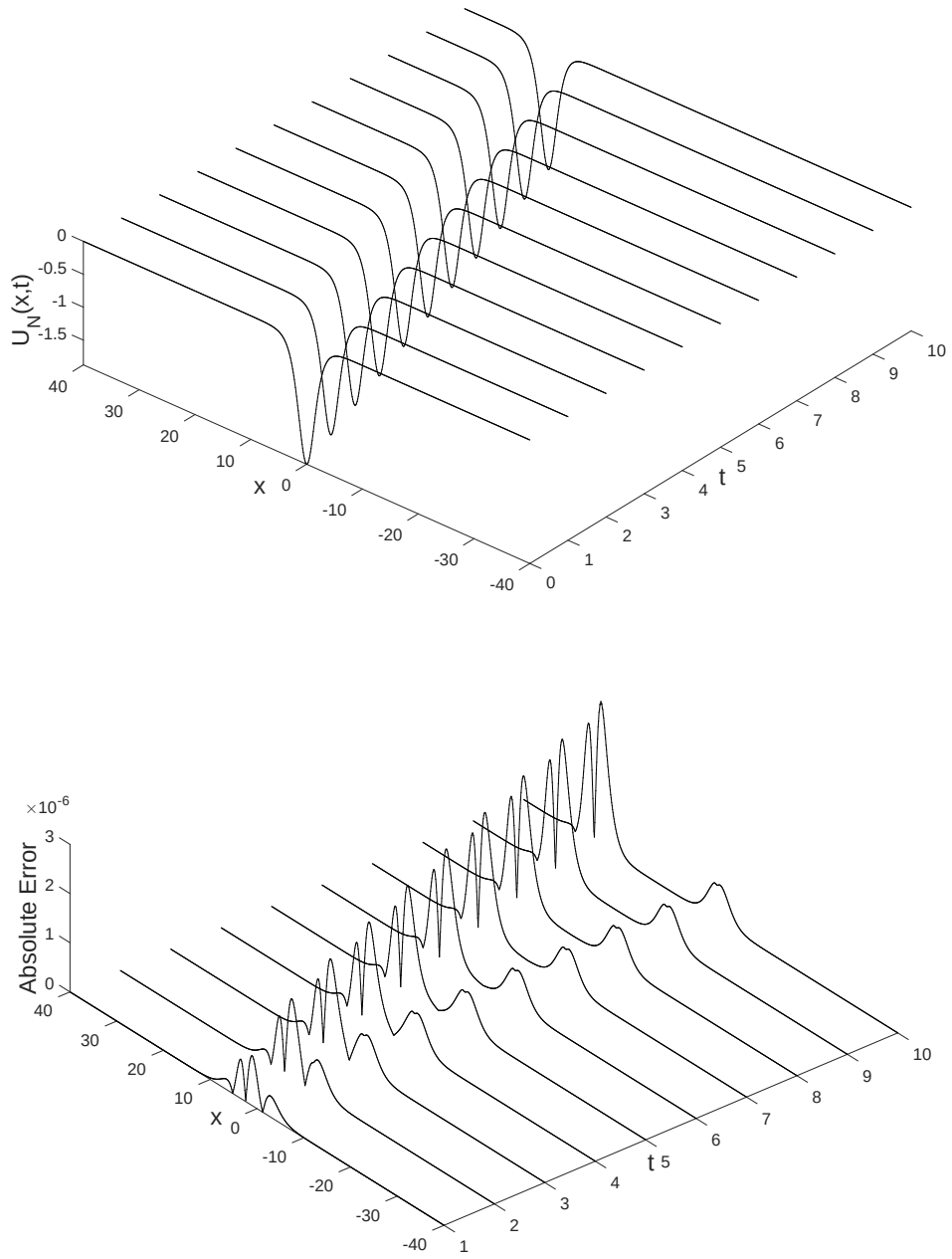

Figure 2: Soliton wave progression (*upper*) and absolute error (*bottom*) of the mDP equation for $h = 0.1,\ \Delta t = 0.001$

method. The presented method's efficiency and power were demonstrated by comparing the values of the numerical and the exact solution at various times and positions, in addition to the calculation of the error norms L_2 and L_∞. The numerical results calculated were compared with the [16] study using the quartic B-spline collocation method. The results indicate that the absolute error found in the proposed method is significantly smaller than those found in the [16]. As can be seen from the Tables 1 and 4, the soliton wave resulting from the solution of the mDP equation moves faster than the soliton wave formed by the solution of mCH. It has been observed that the applied method preserves the physical structure of the solution very well, and it is also speedy and effective since tiny h and Δt are not used.

Declaration of Ethical Standards

The author declares that the materials and methods used in his study do not require ethical committee and/or legal special permission.

Conflicts of Interest

The author declares no conflict of interest.

References

[1] Abbasbandy S., *Solitary wave solutions to the modified form of Camassa–Holm equation by means of the homotopy analysis method*, Chaos, Solitons and Fractals, 39, 428-435, 2009.

[2] Ali I., Haq S., Hussain M., Nisar K.S., Arifeen S.U., *On the analysis and application of a spectral collocation scheme for the nonlinear two-dimensional fractional diffusion equation,* Results in Physics, 56, 1-11, 2024.

[3] Behera R., Mehra M., *Approximate solution of modified Camassa–Holm and modified Degasperis–Procesi equations using wavelet optimized finite difference method*, International Journal of Wavelets, Multiresolution and Information Processing, 11(2), 1-13, 2013.

[4] Camassa R., Holm D.D., *An integrable shallow water equation with peaked solitions*, Physical Review Letters, 71, 1661-1664, 1993.

[5] Degasperis A., Procesi M., Asymptotic Integrability. In: Degasperis A., et al., Eds., Symmetry and Perturbation Theory, World Scientific, 23-37, 1999.

[6] Ganji D.D., Sadeghi E.M.M., Rahmat M.G., *Modified forms of Degaperis-Procesi and Camassa-Holm equations solved by Adomian's decomposition method and comparison with HPM and exact solution*, Acta Applicandae Mathematicae, 104, 303-311, 2008.

[7] Keskin P., *Trigonometric B-spline solutions of the RLW equation*, Ph D., Eskişehir Osmangazi University, Eskişehir, Türkiye, 2017.

[8] Liu Z., Ouyang Z., *A note on solitary waves for modified forms of Camassa–Holm and Degasperis–Procesi equations*, Physics Letters A, 366(4-5), 377-381, 2007.

[9] Logan D.L., A First Course in the Finite Element Method (Fourth Edition), Thomson, 2007.

[10] Lundmark H., Szmigielski J., *Multi-peakon solutions of the Degasperis–Procesi equation*, Inverse Problems, 19(6), 1241-1245, 2003.

[11] Manafian J., Shahabi R., Asaspour M., Zamanpour I., Jalali J., *Construction of exact solutions to the modified forms of DP and CH equations by analytical methods*, Statistics, Optimization and Information Computing, 3, 336-347, 2015.

[12] Mustafa O.G., *A note on the Degasperis–Procesi equation*, Journal of Mathematical Physics, 12(1), 10-14, 2005.

[13] Rao Singiresu S., The Finite Element Method in Engineering (Fifth Edition), Elsevier, 2011.

[14] VonNeumann J., Richtmyer R.D., *A method for the numerical calculation of hydrodynamic shocks*, Journal of Applied Physics, 21, 232-237, 1950.

[15] Walz G., *Identities for trigonometric B-splines with an application to curve design*, BIT Numerical Mathematics, 37, 189-201, 1997.

[16] Wasim I., Abbas M., Iqbal M.K., *Numerical solution of modified forms of Camassa-Holm and Degasperis-Procesi equations via quartic B-spline collocation method*, Communications in Mathematics and Applications, 9(3), 393-409, 2018.

[17] Wang Q., Tang M., *New exact solutions for two nonlinear equations*, Physics Letters A, 372(17), 2995-3000, 2008.

[18] Wazwaz A.M., *New solitary wave solutions to the modified forms of Degasperis–Procesi and Camassa–Holm equations*, Applied Mathematics and Computation, 186, 130-141, 2007.

[19] Wazwaz A.M., *Solitary wave solutions for modified forms of Degasperis–Procesi and Camassa–Holm equations*, Physics Letters A, 352(6), 500-504, 2006.

[20] Yousif M.A., Mahmood B.A., Easif F.H., *A new analytical study of modified Camassa-Holm and Degaperis-Procesi equations*, American Journal of Computational Mathematics, 5, 267-273, 2015.

[21] Yusufoglu E., *New solitonary solutions for modified forms of DP and CH equations using Exp-function method*, Chaos, Solitons and Fractals, 39(5), 2442-2447, 2009.

[22] Zada L., Nawaz R., *An Efficient approach for solution of Camassa-Holm and Degasperis-Procesl equations*, UPB Scientific Bulletin, Series D: Mechanical Engineering, 79(3), 25-34, 2017.

[23] Zhang B.G., Li S.Y., Liu Z.R., *Homotopy perturbation method for modified Camassa-Holm and Degasperis-Procesi equations*, Physics Letters A, 372(11), 1867-1872, 2008.

[24] Zhang B.G., Liu Z.R., Mao J.F., *New exact solutions for mCH and mDP equations by auxiliary equation method*, Applied Mathematics and Computation, 217, 1306-1314, 2010.

[25] Zhou Y., *Blow-up phenomenon for the integrable Degasperis–Procesi equation*, Physics Letters A, 328(2-3), 157-162, 2004.